# EVOLUTION IN THE DESIGN OF V-SHAPED HIGHLY CONDUCTIVE PATHWAYS FOR MAXIMUM COOLING A HEAT-GENERATING PIECE ACCORDING TO CONSTRUCTAL THEORY

M. R. Hajmohammadi[1], G. Lorenzini[2], S. S. Nourazar[1] and C. Biserni[3]

[1]Department of Mechanical Engineering, The University of Texas at San Antonio, San Antonio, Texas 78249, USA

[2]Dipartimento di Ingegneria Industriale, Università degli Sudi di Parma, Parco Area delle Scienze 181/A, 43124 Parma, Italy

[3]Dipartimento di Ingegneria Industriale, Università degli Studi di Bologna, Viale Risorgimento 2, 40136 Bologna, Italy

**Abstract**

This paper presents the evolution of architecture of high conductivity pathways embedded into a heat generating body on the basis of Constructal theory. The main objective is to introduce new geometries for the highly conductive pathways, precisely configurations shaped as V. Four types of V-shaped inserts, evolving from 'V1' to 'V4', have been comparatively considered. Geometric optimization of design is conducted to minimize the peak temperature of the heat generating piece. Many ideas emerged from this work: first of all, the numerical results demonstrated that the V-shaped pathways remarkably surpass the performance of some basic configurations already mentioned in literature, i.e. "I and X-shaped" pathways. Furthermore, the evolution of configurations from 'V1' to 'V4' resulted in a gradual reduction of the hot spot temperature, according to the principle of "optimal distribution of imperfections" that characterizes the constructal law.

**Keywords:** Thermal performance, Electronic cooling, High conductivity, Optimum design

**Nomenclature**

A area, $m^2$

D length, m

H height, m

k thermal conductivity, W $m^{-1}$ $K^{-1}$

n coordinate normal to the surface, m

q''' heat generation rate per unit volume, W $m^{-3}$

T local temperature, K

V volume, $m^3$

W width, m

x,y cartesian coordinates, m

**Greek symbol**

ω volume fraction of the insert

λ thermal conductivity ratio

**Superscripts**

( ˜ ) dimensionless variables

**Subscripts**

a auxiliary part of the insert

h high conductivity insert

i inclined part of the insert

l low conductivity material

m middle part of the insert

max maximum

min minimum

opt optimized

ref reference

## 1. Introduction

Constructal theory and design [1-4] have emerged as the evolutionary design philosophy for developing flow architectures that offer greater flow access and system performance. In this context, fins and cavities [5-13], convective micro-channels [14-18] and highly conductive inserts [19-29] drew more attentions. Other possible interdisciplinary applications of constructal theory are treated in Refs.[30] and [31].

Fins are frequently used in engineering to enhance the rate of heat transfer on a solid surface: an optimization analysis has been performed by Almogbel in Ref. [5] with the purpose to maximize the global thermal conductance of tree-shaped fins subject to total volume and fin material constraints. Almogbel and Bejan in Ref. [6] studied a T-shaped assembly of plate fins, for which they showed that the constructal optimization of shape can lead to substantial increases in global conductance. More recently, Lorenzini and Rocha carried out a numerical work [11] to discover the best geometry of a T–Y assembly of fins. Hajmohammadi et Al. in Ref. [13] demonstrated that by using several branches of equal cavities, the heat generating body operates at the lower level of the peak temperature when compared with C-, T- and H-shaped cavities.

Microchannel heat sinks were first introduced by Tuckerman and Pease [14, 15]. They used direct water circulation in fabricated microchannels and showed that these kinds of cooling systems may be a practical solution for compact devices requiring high rates of heat removal. Wang et al. in Ref. [16] investigated fluid flow and heat transfer characteristics in branching networks built into heat sinks. One fascinating feature of tree networks for fluid flow is that they are not only present in engineering, i.e., man-made architectures, but also occur abundantly in natural flow systems, e.g., respiratory airways [30] and river basins [31]. However, in man-made

engineering networks for fluid flows, the pumping power to be provided and the minimization of the pressure drop are the elements of major concern. The conductive pathways of high-conductivity inserts with low occupancy have been proposed to overcome the forgoing concerns associated with fluid flow networks. Highly conductive cooling inserts become a necessity as the cooling and sensing of smart materials marches toward smaller scales and higher densities of functionality. The challenge that emerges with designing the high conductivity inserts is to optimize the architecture of the paths for heat removal from a low conductive domain (electronic component). For example, Almogbel and Bejan in Ref. [20] proposed a non-uniformly distribution of high conductive material and achieved a remarkable improvement in the global performance. Optimal configurations of highly conductive materials at micro- and nano-scales were proposed by Gosselin and Bejan in Ref. [25]. Discrete variable cross-section conducting paths of inserts were illustrated by Wei et Al. in Ref. [27]. Most recently, Lorenzini et Al. in Ref. [29] carried out the optimization of conductive inserts by introducing X-shaped pathways of higher thermal conductivity. In this context, the present study can be considered as an evolution of the geometrical optimization performed in Ref. [29]: four types of V-shaped conductive pathways, evolving from 'V1' to 'V4' inserts, have been introduced. The problem statement here treated, with reference to the electronic devices field, can be illustrated as follows: consider designing a package of electronic components, which must fit inside a given volume, i.e., the global constraint. The objective of the design is to install as much circuitry as possible in this volume. Because electrical components generate heat, this objective is equivalent to installing as much heat generation rate as possible. The highest temperature in the package, i.e., the hot spot, must not exceed a specified threshold: this becomes the local constraint, or the "allowable peak of imperfection".

## 2. Physical problem: V-shaped conductive pathways

Consider the two-dimensional heat generating bodies intruded by high conductivity pathways highlighted in Figure 1: four geometrical configurations, evolving from 'V1' to 'V4'

have been studied. The external dimension is (H) for the square piece, ($D_i$, $H_i$, α) for the 'V1' insert, ($D_i$, $H_i$, $D_m$, $H_m$, α) for the 'V2' insert, ($D_i$, $H_i$, $H_a$, α) for the 'V3' insert and ($D_i$, $H_i$, $D_m$, $H_m$, $H_a$, α) for the 'V4' insert. As illustrated in Fig.1, each insert consists of some components, for example, the inclined part, the middle part, or the auxiliary, shown by subscripts: 'i', 'm' and 'a', respectively. For example, '$D_i$' is a dimension associated with inclined parts of the insert. The total volume occupied by the entire system (heat generating body and insert) is fixed,

$$V_{tot} = V_l + V_h = H^2 W = Const. \tag{1}$$

Where the subscript l is referred to the low conductivity material (heat generating body) and h to the high conductivity materials (insert). W is the thickness of the body, perpendicular to the plane of Fig. 1. For the sake of simplicity, the variability of all parameters along the W dimension is assumed negligible. Thus, the area of square body, $A_{tot} = H^2$ can also be considered fixed. The volume/area occupied by the insert is fixed as well, i.e.

$$\begin{aligned} A_h &= A_i = Const. && \text{(V1) type} \\ A_h &= A_i + A_m = Const. && \text{(V2) type} \\ A_h &= A_i + A_a = Const. && \text{(V3) type} \\ A_h &= A_i + A_m + A_a = Const. && \text{(V4) type} \end{aligned} \tag{2}$$

The volume constraints (1) and (2) are expressed by the relations,

$$\begin{aligned} \omega &= \frac{A_h}{A_{tot}} = \frac{A_i}{A_{tot}} = \omega_i = Const. && \text{(V1) type} \\ \omega &= \frac{A_h}{A_{tot}} = \frac{A_i + A_m}{A_{tot}} = \omega_i + \omega_m = Const. && \text{(V2) type} \\ \omega &= \frac{A_h}{A_{tot}} = \frac{A_i + A_a}{A_{tot}} = \omega_i + \omega_a = Const. && \text{(V3) type} \\ \omega &= \frac{A_h}{A_{tot}} = \frac{A_i + A_m + A_a}{A_{tot}} = \omega_i + \omega_m + \omega_a = Const. && \text{(V4) type} \end{aligned} \tag{3}$$

where, ω represents the volume fraction occupied by the high conductivity materials (insert). The solid is assumed isotropic with constant thermal conductivity, $k_l$, and generates heat uniformly at the volumetric rate q''' [W/m$^3$]. The outer surfaces of the heat generating body are perfectly insulated. The generated heat current (q'''$A_l$) is removed by the high conductivity materials with constant thermal conductivity, $k_h$, to a heat sink at the minimum temperature level, $T_{min}$ located in the rim (heat sink). Due to the high conduction resistance of the heat generating body, the temperature level in the body rises to levels higher than the minimum temperature in the rim. Such highest temperatures (the 'hot spots') are normally registered at points on the insulated perimeter. The peak temperature of the body may exceed the allowable temperature level. Knowing that the performance of equipment has a direct relationship with its temperature, it is important to keep the hot spot temperature not exceeding a specified threshold. Therefore, the design objective is represented by the minimization of the global thermal resistance ($T_{max} - T_{min}$)/(q'''A). The numerical optimization of geometric parameters of the insert consist of calculating the temperature field in a large number of configurations (with different geometric parameters of the V-shaped insert), determining the global thermal resistance for each configuration, and selecting the configuration with the smallest global resistance. Symmetry allowed us to perform calculations in only half of the domain.

## 3. Mathematical formulation and numerical solution

The 2-D conduction equation for the domain occupied by the heat generating body under steady-state conditions is,

$$\frac{\partial^2 \tilde{T}_l}{\partial \tilde{x}^2} + \frac{\partial^2 \tilde{T}_l}{\partial \tilde{y}^2} + 1 = 0. \tag{4}$$

where the dimensionless variables and parameters are defined as,

$$\tilde{T} = \frac{T - T_{min}}{q''' A_{tot} / k_l} \tag{5}$$

and,

$$(\tilde{x},\tilde{y},\tilde{n}) = \frac{(x,y,n)}{A_{tot}^{1/2}} \tag{6}$$

while n represents the coordinate normal to the interface surfaces (between the insert and the heat generating body). Herein, the geometric scale is $A_{tot}^{1/2}$ and the temperature scale is an equivalent temperature $q'''A_{tot}/k_l$. The 2-D conduction equation for the domain occupied by the high conductivity materials with no heat generation under steady-state conditions is,

$$\frac{\partial^2 \tilde{T}_h}{\partial \tilde{x}^2} + \frac{\partial^2 \tilde{T}_h}{\partial \tilde{y}^2} = 0. \tag{7}$$

The boundary condition in the rim is, $\tilde{T}_h = 0.$ Continuity in temperature and heat flux at the interface gives,

$$\begin{aligned} &\tilde{T}_l = \tilde{T}_h \\ &\frac{\partial \tilde{T}_l}{\partial \tilde{n}} = \lambda \frac{\partial^2 \tilde{T}_h}{\partial \tilde{n}} \end{aligned} \tag{8}$$

Where $\lambda = k_h / k_l$ is the thermal conductivity ratio.

The optimization objective corresponds to the minimization of the dimensionless peak temperature,

$$\tilde{T}_{max} = \frac{T_{max} - T_{min}}{q''' A_{tot} / k_l}. \tag{9}$$

by relaxing all independent geometric parameters of the 'V1' insert, ($\frac{D_i}{H_i}, \alpha$ ), those of the 'V2' insert, ($\frac{D_i}{H_i}, \frac{D_m}{H_m}, \alpha, \omega_m$), those of the 'V3' insert, ($\frac{D_i}{H_i} \alpha, \omega_a$ ) and those of the 'V4' insert, ($\frac{D_i}{H_i}, \frac{D_m}{H_m}, \alpha, \omega_m, \omega_a$ ). Equations (4) and (7) subject to the set of boundary conditions were solved numerically.

The numerical simulation here performed is based on a finite element analysis developed in the platform of Elmer (an open-source finite element code for multi-physics problems), which

processes partial differential equations in a discrete form and handles the coupled systems of partial differential equations. The element layout is non-uniform in x and y coordinates, and varied from one geometry to the next. Because two different materials are used, it was necessary to use two-level grids with different size steps for the heat generating body and the insert. The appropriate mesh size was determined by means of successive refinements, increasing the number of elements between consecutive mesh sizes, until the strongest convergence criterion was satisfied. Based on the complexity of the cases, about 25,000 to 40,000 grids were used in the simulations. In the case of an I-shaped pathway, numerical tests showing the achievement of grid independence are presented in Table (1), where the numerical results here obtained in Elmer ambient have been compared with the ones obtained by Almogbel and Bejan in Ref. [21] using the MATLAB PDE toolbox.

Table 1. Numerical tests showing the achievement of grid independence with reference to the case of a I-shaped pathway with $\omega = 0.1$, $\lambda = 300$ and the aspect ratio of the insert $D_b / H_b = 0.11$.

| Number of elements | $\tilde{T}_{max}$ | $\left\|\left(\tilde{T}_{max} - \tilde{T}_{max}\ \mathrm{Ref.[21]}\right)/\tilde{T}_{max}\ \mathrm{Ref.[21]}\right\|$ % |
|---|---|---|
| 408 | 0.1245947 | 0.32 |
| 1632 | 0.1247514 | 0.2 |
| 6528 | 0.1248217 | 0.14 |
| 26112 | 0.1248781 | 0.1 |

## 4. Optimization results and discussion

In this section, first and foremost, the optimization results addressing the optimal geometry of the high conductive pathways and the corresponding reduction in excess temperature of the heat generating body are presented with reference to the four cases, involving the configurations named 'V1', 'V2', 'V3' and 'V4'. Second, the minimum peak temperatures, obtained in V-shaped patterns have been compared among the minimum peak temperatures obtained for the I-shaped insert [21] and those obtained for the latest pattern (X-shaped) [29] introduced in literature.

The optimization process is carried out in several levels. In each level of optimization, the peak temperature, $\tilde{T}_{max}$, is minimized with reference to the variation of a new variable, in addition to the preceding ones. The minimized peak temperature, $\tilde{T}_{max}$, receives new subscript 'm' (representing 'minimized') and the new variable, as well as the preceding variables, receive new subscript 'o' (representing 'optimized'). For example, if η and ξ are two optimization variables, "$\tilde{T}_{max})_m$ and $\eta_o$" characterize the first level of optimization, where $\tilde{T}_{max}$ is minimized once with respect to η variation while "$\tilde{T}_{max})_{mm}, \xi_o$ and $\eta_{oo}$" characterize the second level of optimization, where $\tilde{T}_{max}$ is minimized twice with respect to ξ variation in addition to variation of η. In the last level of optimization, the minimum peak temperature, $\tilde{T}_{max})_{min}$ is achieved. The influence of the angle α (see Fig. 1 for geometry definition) on the peak temperature of the heat generating body intruded by a 'V1' insert, is shown in Figs. 2 and 3, respectively, for several values of high conductivity materials volume fraction, ω, and for several values of the thermal conductivity ratio, λ. During this first step of the optimization procedure, a fixed value of the aspect ratio $D_1/H_1$ (i.e.$D_1/H_1 = 0.3$) has been considered. Based on pure observation, we discovered that there is an optimal α which minimizes $\tilde{T}_{max}$. The dimensionless temperature $\tilde{T}_{max}$ also decreases, as expected, when ω and λ increase. The procedure of figs. 2 and 3 is repeated in Fig. 4 for a wide range of $D_1/H_1$, when $\omega = 0.2$ and $\lambda = 100$: there is an optimal value of $D_1/H_1$ which minimizes the parameter $\tilde{T}_{max})_{min}$ with respect to α. The results of last level of the optimization process are shown in Fig. 5, where the peak temperature is minimized with reference to all independent

geometric parameters of the 'V1' insert. In the diagram at the bottom of Fig. 5, the performance indicators of the 'V1' configuration, i.e. the minimum peak temperatures achieved in the last optimization level, have been compared with those referred to the I-shaped insert [21] and to the X-shaped pathway [29]. It is evident that 'V1' configurations perform better than I-shaped and X-shaped intrusions in lowering the peak temperatures. The superiority of 'V1' insert versus X-shaped model becomes even more manifest for the lower values of ω. For example, when ω =0.05 and λ = 100, the minimum peak temperature is approximately 20 % better if compared with the one calculated in the X-shaped geometry. On the contrary, the peak temperatures are practically the same and prove to be insensible to geometry ('V1' and/or X-shaped inserts) if ω =0.2 and λ = 100. Let now assume that the 'V1' insert evolves to the 'V2' configuration, which has an extra middle part, as highlighted in Fig.1. Displayed in Figure 6 is the third level of optimization, where $\tilde{T}_{max}$ is optimized with respect to the parameters α, $D_i/H_i$ and $D_m/H_m$ for a wide range of $\omega_m$ (the subscript 'm' means referred to the middle part of the insert). The main outcome is that the 'middle insert', that has been added to the 'V1' configuration to obtain the 'V2' pathway, has a sensible effect in reducing the peak temperatures. This assumption is confirmed in Figure 7 where a comparison regarding all the tested geometries ('V1'insert, 'V2'insert, I-and X shaped pathways) is illustrated. For example, when ω =0.2 and λ = 100, the minimum peak temperature referred to the 'V2' configuration is 13 % better than the X-shaped construct. Besides, when ω = 0.05, λ = 100 and the V-shaped insert evolves from 'V1' to 'V2', the efficiency of the V-shaped insert over the X-shaped intrusion rises from 20% to 23 %.

Now consider that the 'V1' insert evolves to the 'V3' configuration, which has an extra auxiliary part, as sketched in Fig.1. Figure 8 shows that the optimization opportunity described for $\omega_m$ in Fig. 6, also holds for the auxiliary inserts, i.e., there is an optimal $\omega_a$ ('a' represents the auxiliary part) which minimizes the peak temperature in the 'V3' case. The comparison between the performance of the 'V3' insert and the previous ones is made in Fig. 9. It is observed that the 'V3' insert, as well as the 'V2' insert, performs better than the 'V1' insert and those configurations considered in literature. Besides, the 'V3' insert is superior than 'V2' insert,

provided that ω exceeds 0.12. For example, when ω = 0.2 and λ = 100, the minimum peak temperature is about 25 % better than the X-shaped,: this value is considerably augmented if we take into account the previous value of 13%, reported for the 'V2' type under the same circumstances of ω and λ. The final efforts for improving and evolving the V-shaped inserts here treated are made by using both middle and auxiliary parts, which characterize the V-shaped pathways named 'V4'. In this sense, Figure 10 characterize the full optimization results for the 'V4' insert. Comparison among the minimized temperatures reveals that the performance of the 'V4' type is remarkably enhanced and it is more efficient than the other configurations in reducing the peak temperature. For example, when λ =100 and ω = 0.2, 'V4' insert is about 15% better than the 'V3' insert. In this case, the minimum temperature achieved in 'V4' case is about 40 % lower than the one reported for the X-type. This is a remarkable achievement and may be notable for engineers engaged in the related design. To underline the advantage of using V-shaped inserts over the configurations mentioned in literature [21 and 29], another comparison scheme is performed in Fig. 11 where it is assumed that $\tilde{T}_{max}$ is a constraint and the minimization of the insert volume fraction, ω, is the objective. The simulation results illustrated in Fig. 11 are referred to the cases of λ =100 and λ =300. When λ =100 and the peak temperature is a constraint at $\tilde{T}_{max}$=0.06, it is observed that the use of a 'V4' insert having ω = 0.105 is equivalent to the use of a X-shaped insert with ω = 0.19. This means that a X-shaped insert and a 'V4' insert with almost half amount of the high conductivity material used for the X-shaped pathway, present the same peak temperatures. It is worth adding that the achievements are more pronounced when the very high conductivity materials (λ =300) are utilized. In this case, Fig. 11 reveals that a 'V4' insert with almost one third amount of the high conductivity materials used for the X-shaped insert can compete the X-shaped insert in lowering the hot spots (peak) temperatures. For sake of clarity, the optimal shapes referred to several investigated configurations are shown in scale in Fig. 12. Figure 12 also highlights how the hot spots move from one configuration to the other, according to the principle of "optimal distributions of imperfections" that characterizes Bejan's Theory.

## 5. Conclusions

In the present work, we carried out a numerical investigation on new geometries of conductive inserts, consisting in V-shaped pathways that intrude into a heat generating piece. Four types of V-shaped configurations, evolving from 'V1' to 'V4', were introduced. An optimization procedure has been here performed with the purpose to minimize the peak temperature in the heat generating body, by varying the geometric parameters of the inserts. First of all, we discovered that the performance of the V-shaped geometry is superior to the one of I- and X- shaped inserts existing in literature: this become more pronounced depending on the volume fraction of the inserts, $\omega$, and on the thermal conductivity ratio, $\lambda$. We also discovered that the evolution of V-shaped inserts, from 'V1' to 'V4', resulted in a gradual reduction of the peak temperatures, in accordance with the principle of "optimal distribution of imperfections" that characterizes the constructal law. For example, when $\omega = 0.2$ and $\lambda = 100$, 'V4' insert performs approximately 15% better than 'V3' geometry. Furthermore, the minimum temperature achieved with reference to the 'V4' configuration proved to be nearly 40 % lower than the one calculated in the X-shaped insert.

**Acknowledgements** Professor Giulio Lorenzini and Professor Cesare Biserni were funded by Italian MIUR.

## References

[1] A. Bejan, Advanced Engineering Thermodynamics, second ed., Wiley, New York, 1997.

[2] A. Bejan, Shape and Structure, from Engineering to Nature, Cambridge University Press, Cambridge, UK, 2000.

[3] A.H. Reis, Constructal theory: from engineering to physics and how flow systems develop shape and structure, Appl. Mech. Rev. 59 (2006) 269–282.

[4] A. Bejan and S. Lorente, Design with Constructal Theory, Wiley, Hoboken, 2008.

[5] M. Almogbel, Constructal tree-shaped fins, Int. J. Thermal Sciences, 44 (2005) 342–348.

[6] M. Almogbel, A. Bejan, Cylindrical Trees of Pin Fins, Int. J. Heat Mass Transfer, 43 (2000) 4285–4297.

[7] T. Bello-Ochende, J.P. Meyer, A. Bejan, Constructal multi-scale pin–fins, Int. J. Heat Mass Transfer, 53 (2010) 2773–2779.

[8] A. Bejan, M. Almogbel, Constructal T-Shaped Fins, Int. J. Heat Mass Transfer, 43 (2000) 2101–2115.

[9] B. Kundu, D. Bhanja, Performance and optimization analysis of a constructal T-shaped fin subject to variable thermal conductivity and convective heat transfer coefficient, Int. J. Heat Mass Transfer, 53 (2010) 254–267.

[10] G. Lorenzini, L.A.O. Rocha, Constructal Design of Y-Shaped Assembly of Fins, Int. J. Heat Mass Transfer, 49 (2006) 4552–4557.

[11] G. Lorenzini, L.A.O. Rocha, Constructal design of T–Y assembly of fins for an optimized heat removal, Int. J. Heat Mass Transfer, 52 (2009) 1458–1463.

[12] G. Lorenzini, L. Rocha, Geometric optimization of T-Y-shaped cavity according to constructal design, Int. J. Heat Mass Transfer, 52 (2009) 4683–4688.

[13] M.R. Hajmohammadi, S. Poozesh, A. Campo, S.S. Nourazar, Valuable reconsideration in the constructal design of cavities, Energy Conversion and Management, 66 (2013) 33–40.

[14] D.B. Tuckerman, R.F.W. Pease, High-Performance Heat Sinking for VLSI, IEEE Electron Device Letters,, 2 (1981) 126–129.

[15] D.B. Tuckerman, R.F.W. Pease, Ultrahigh Thermal Conductance Microstructures for Integrated Circuits, IEEE Proceedings of the 32nd Electronic Conference, 101 (1982) 145–149.

[16] X.A. Wang, S. Mujumdar, C. Yap, Thermal characteristics of tree-shaped microchannel nets for cooling of a rectangular heat sink, Int. J. Therm. Sciences, 45 (2006) 1103-1112.

[17] P. Naphon, O. Khonseur, Study on the convective heat transfer and pressure drop in the micro-channel heat sink, Int. Communications Heat and Mass Transfer, 36 (2009), 39-44.

[18] I. Tiselj, G. Hetsroni, B. Mavko, A. Mosyak, E. Pogrebnyak, Z. Segal, Effect of axial conduction on the heat transfer in micro-channels, Int. J. Heat Mass Transfer, 47 (2004) 2551-2565.

[19] A. Bejan, Constructal-theory network of conducting paths for cooling a heat generating volume, Int. J. Heat Mass Transfer, 40 (1997) 799–816.

[20] M. Almogbel, A. Bejan, Constructal optimization of nonuniformly distributed tree-shaped flow structures for conduction, Int. J. Heat Mass Transfer, 44 (22) (2001) 4185–4194.

[21] M. Almogbel, A. Bejan, Conduction trees with spacings at the tips, Int. J Heat Mass Transfer, 42(20) (1999) 3739-3756.

[22] G.A. Ledezma, A. Bejan, M.R. Errera, Constructal tree networks for heat transfer, J. Applied Physics, 82(1) (1997) 89-100.

[23] L.A.O. Rocha, S. Lorente, A. Bejan, Constructal design for cooling a disc-shaped area by conduction, Int. J. Heat Mass Transfer, 45(8) (2002) 1643–1652.

[24] L. Ghodoossi, N. Eğrican, Conductive cooling of triangular shaped electronics using constructal theory, Energy Conversion and Management, 45(6) (2004) 811-828.

[25] L. Gosselin, A. Bejan, Constructal heat trees at micro and nanoscales, Journal of Applied Physics, 96(10) (2004) 5852–5859.

[26] L.A.O. Rocha, S. Lorente, A. Bejan, Conduction tree networks with loops for cooling a heat generating volume, Int. J. Heat Mass Transfer, 49 (15–16) (2006) 2626–2635.

[27] S. Wei, L. Chen, F. Sun, The area-point constructal optimization for discrete variable cross-section conducting path, Applied Energy, 86 (7–8) (2009) 1111–1118.

[28] G. Marck, J.L. Harion, M. Nemer, S. Russeil, D. Bougeard, A new perspective of constructal networks cooling a finite-size volume generating heat, Energy Conversion and Management, 52 (2) (2011) 1033-1046.

[29] G. Lorenzini, C. Biserni, L.A.O. Rocha, Constructal design of X-shaped conductive pathways for cooling a heat-generating body, Int. J. Heat Mass Transfer, 58 (2013) 513-520.

[30] A.H. Reis, F. Miguel, M. Aydin, Constructal theory of flow architecture of the lungs, Medical Physics, 31 (2004) 1135–1140.

[31] J.D. Pelletier, D.L. Turcotte, Shapes of river networks and leaves: are they statistically similar?, Philosophical Transactions of the Royal Society, B, 355 (2000) 307–311.

**Figure Captions**

Figure 1 Geometry and coordinate system definition of high conductivity pathways (inserts) intruding a square heat generating piece.

Figure 2 Effects of $\alpha$ on the peak (maximum) temperature of a square piece intruded by a V-shaped insert of 'V1' type for several $\omega$.

Figure 3 Effects of $\alpha$ on the peak temperatures for a 'V1' type of several $\lambda$.

Figure 4 Influence of $D_i$ /$H_i$ on the peak temperatures for a 'V1' type.

Figure 5 Last level of optimization: Optimized parameters related to a V-shaped insert of 'V1' type and the corresponding minimum peak temperatures in comparison with minimum peak temperatures mentioned in literature for other configurations.

Figure 6 Influence of $\omega_m$ on the peak temperature of a heat generating body intruded by a V-shaped insert of 'V2' type.

Figure 7 Comparison of 'V2' with other configurations.

Figure 8 Influence of $\omega_a$ on the peak temperature of a heat generating body intruded by a V-shaped insert of 'V3' type.

Figure 9 Comparison of 'V3' with other configurations.

Figure 10 Comparison of 'V4' with other configurations.

Figure 11 Minimum volume fraction required for maintaining the peak temperature of the heat generating body under an allowable level, $\tilde{T}_{max}$ .

Figure 12 Optimal configurations of V-shaped inserts.

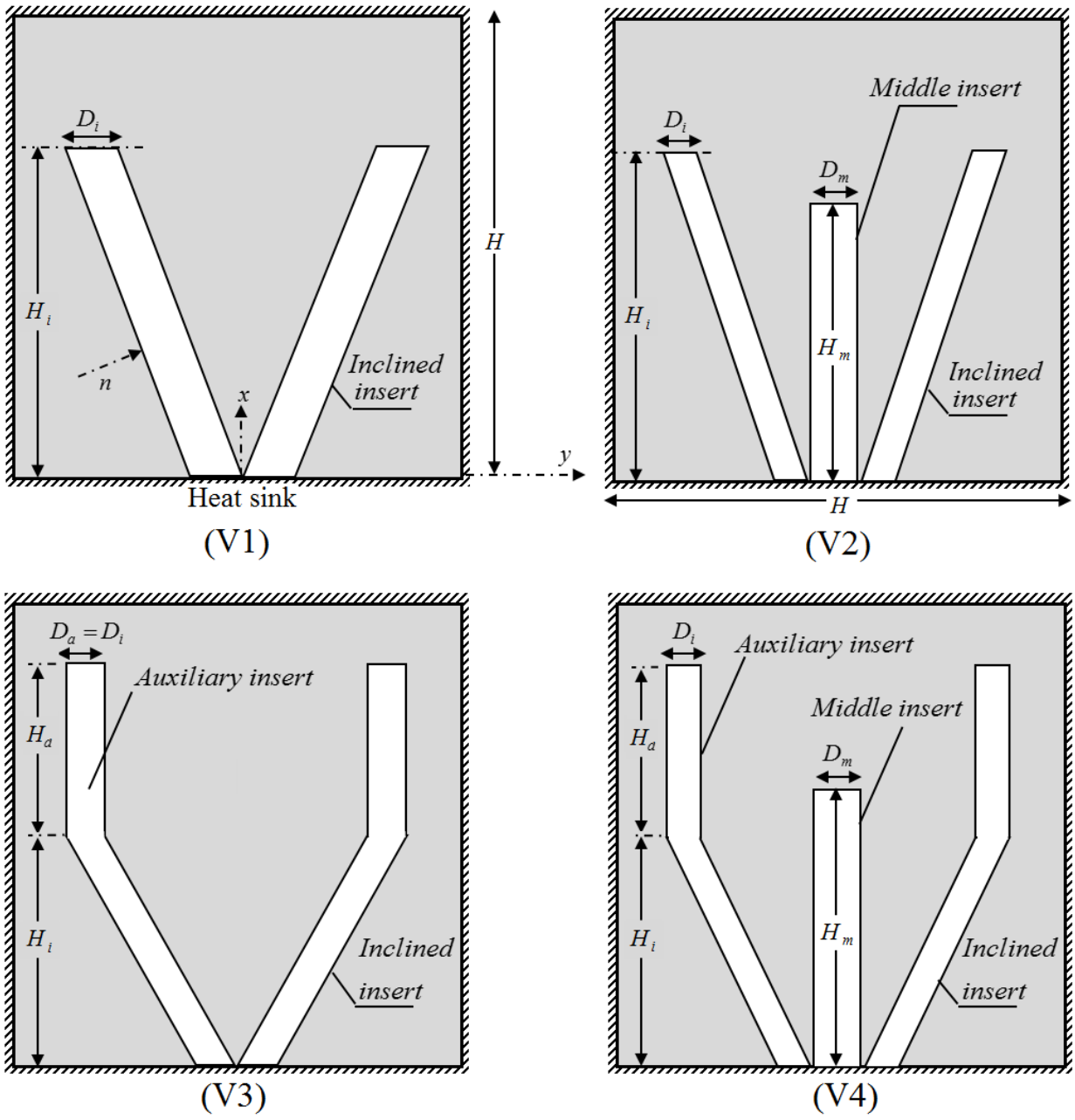


Figure 1 Geometry and coordinate system definition of high conductivity pathways (inserts) intruding a square heat generating piece.

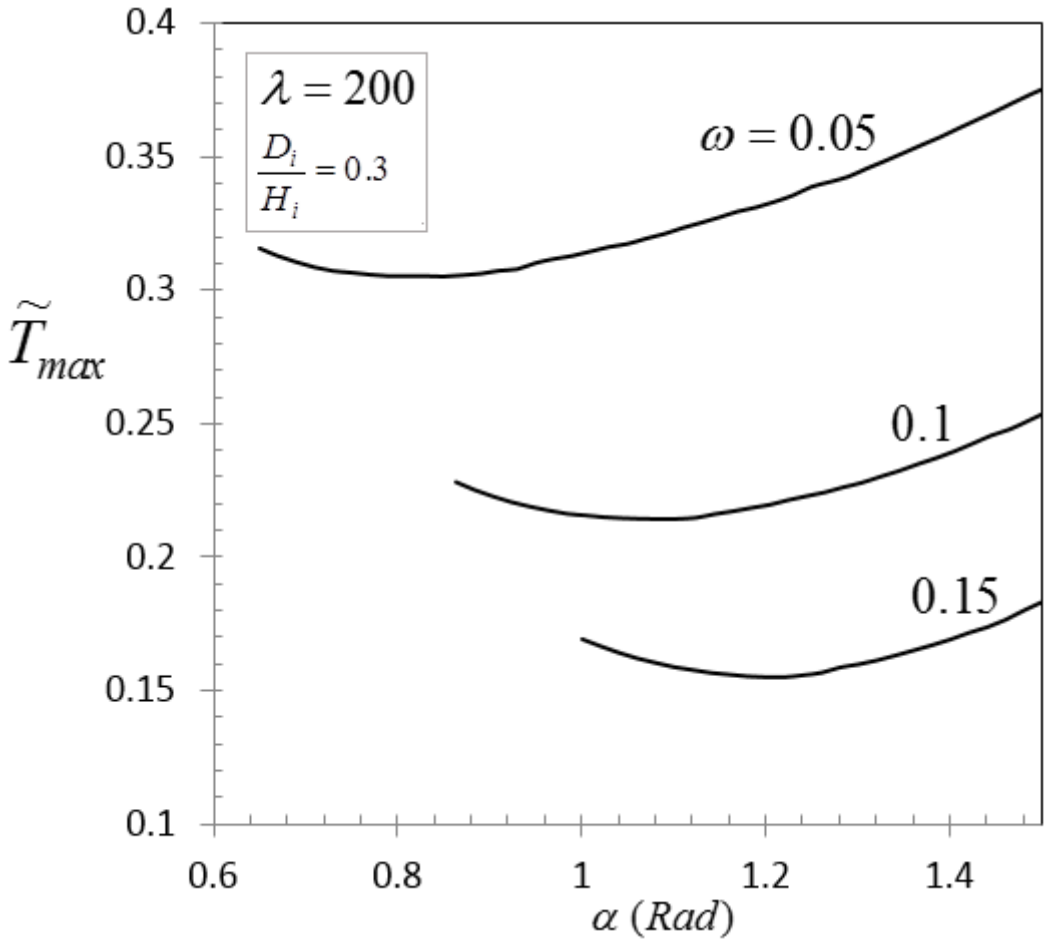


Figure 2 Effects of α on the peak (maximum) temperature of a square piece intruded by a V-shaped insert of 'V1' type for several ω.

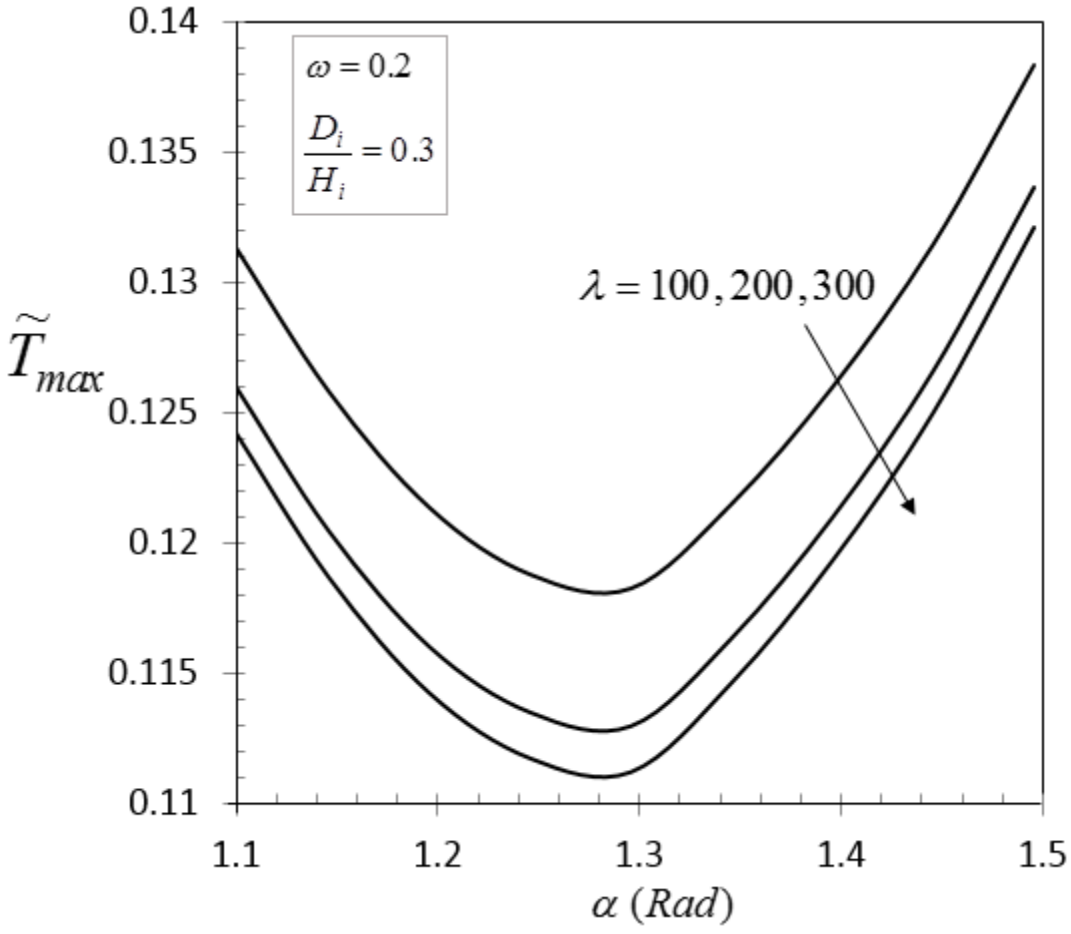


Figure 3 Effects of α on the peak temperatures for a 'V1' type of several λ.

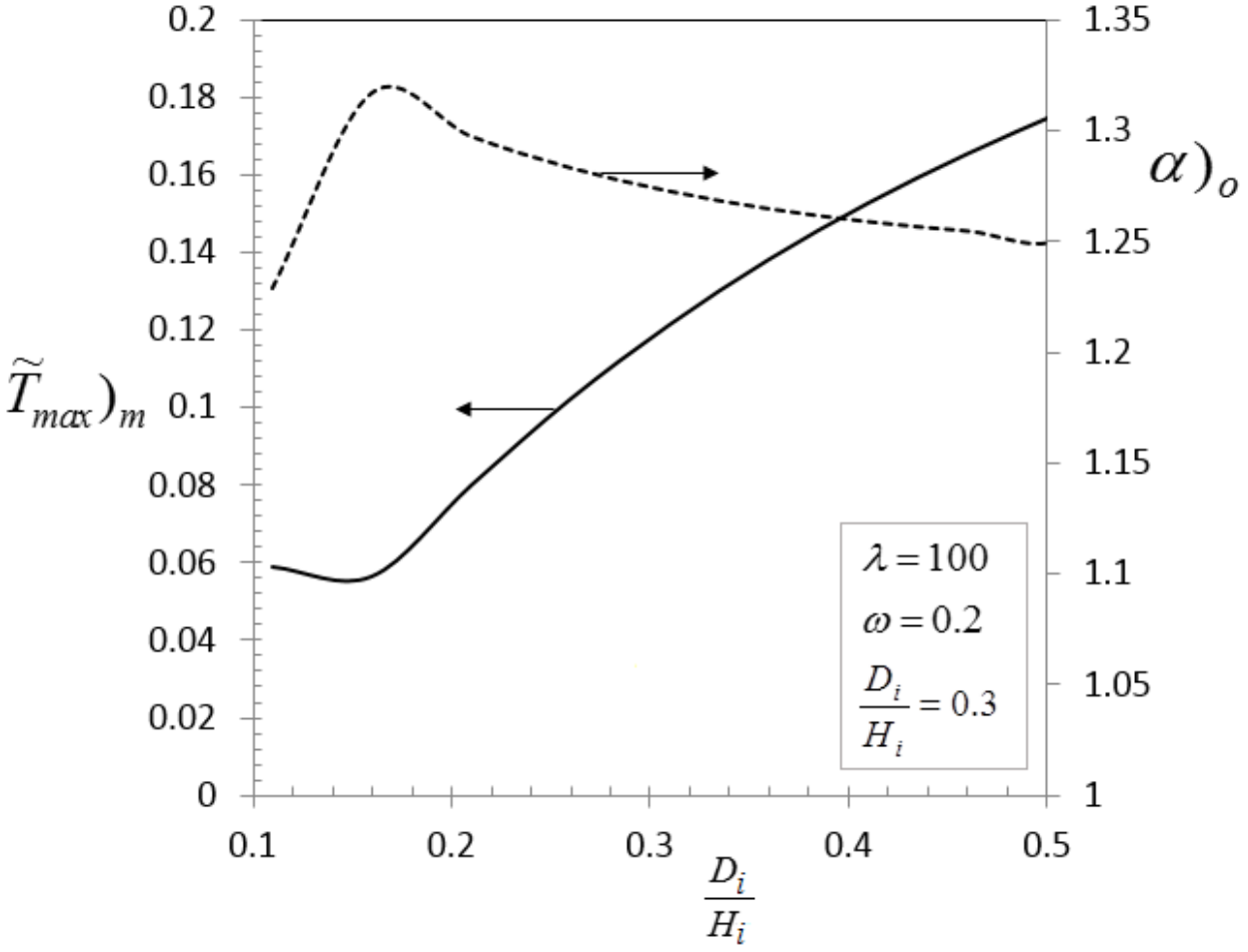


Figure 4 Influence of $D_i$ /$H_i$ on the peak temperatures for a 'V1' type.

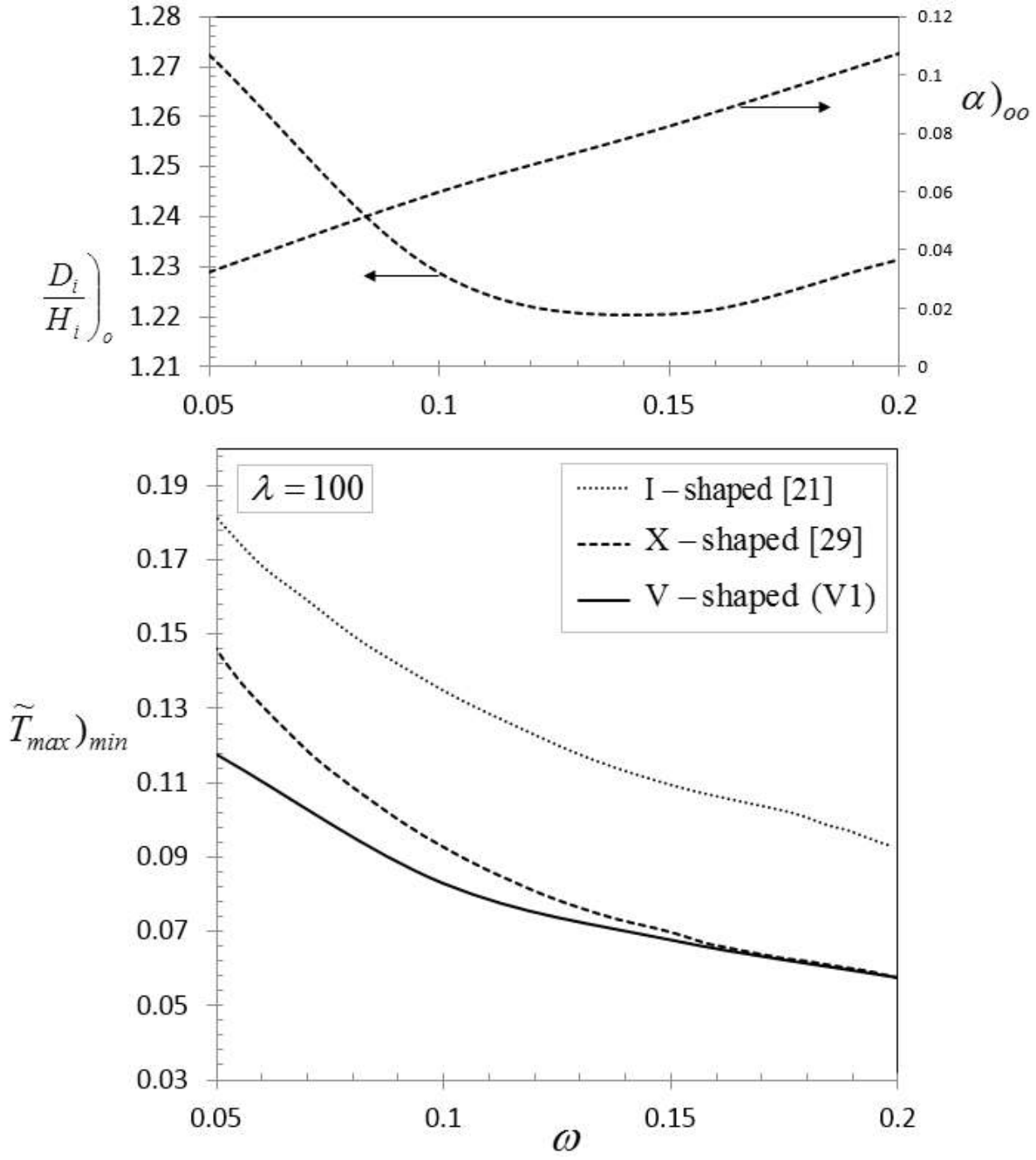


Figure 5 Last level of optimization: Optimized parameters related to a V-shaped insert of 'V1' type and the corresponding minimum peak temperatures in comparison with minimum peak temperatures mentioned in literature for other configurations.

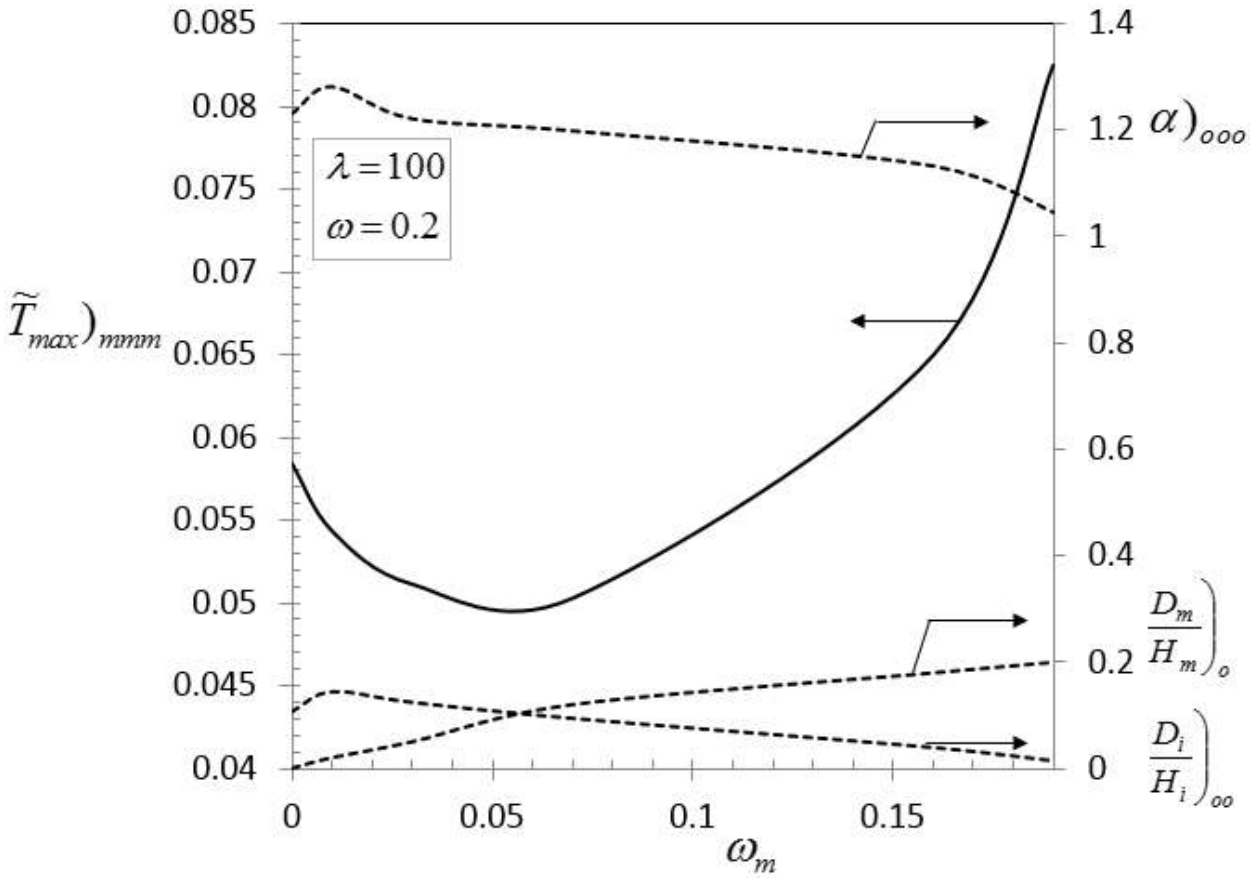


Figure 6 Influence of $\omega_m$ on the peak temperature of a heat generating body intruded by a V-shaped insert of 'V2' type.

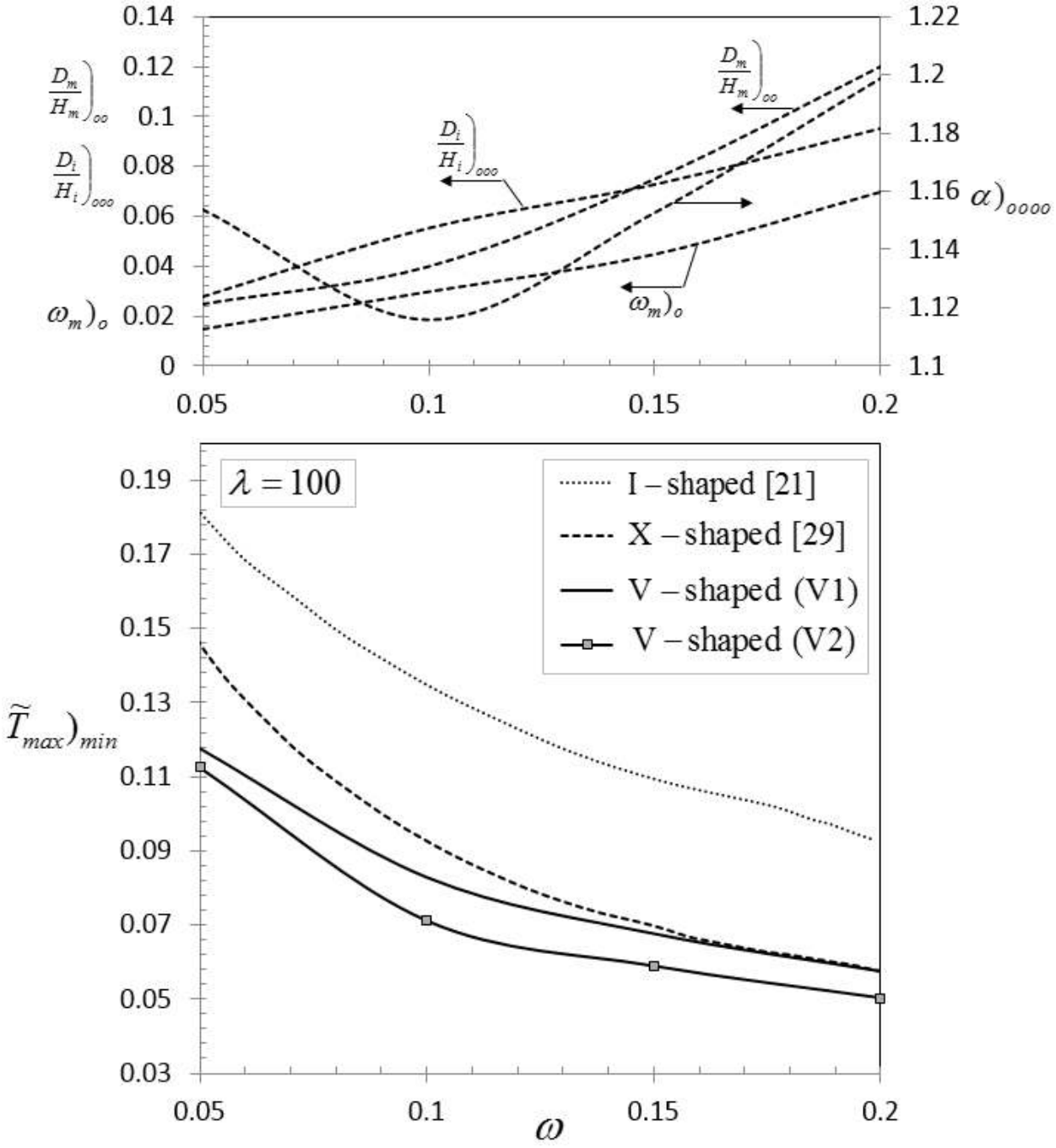


Figure 7 Comparison of ‘V2’ with other configurations.

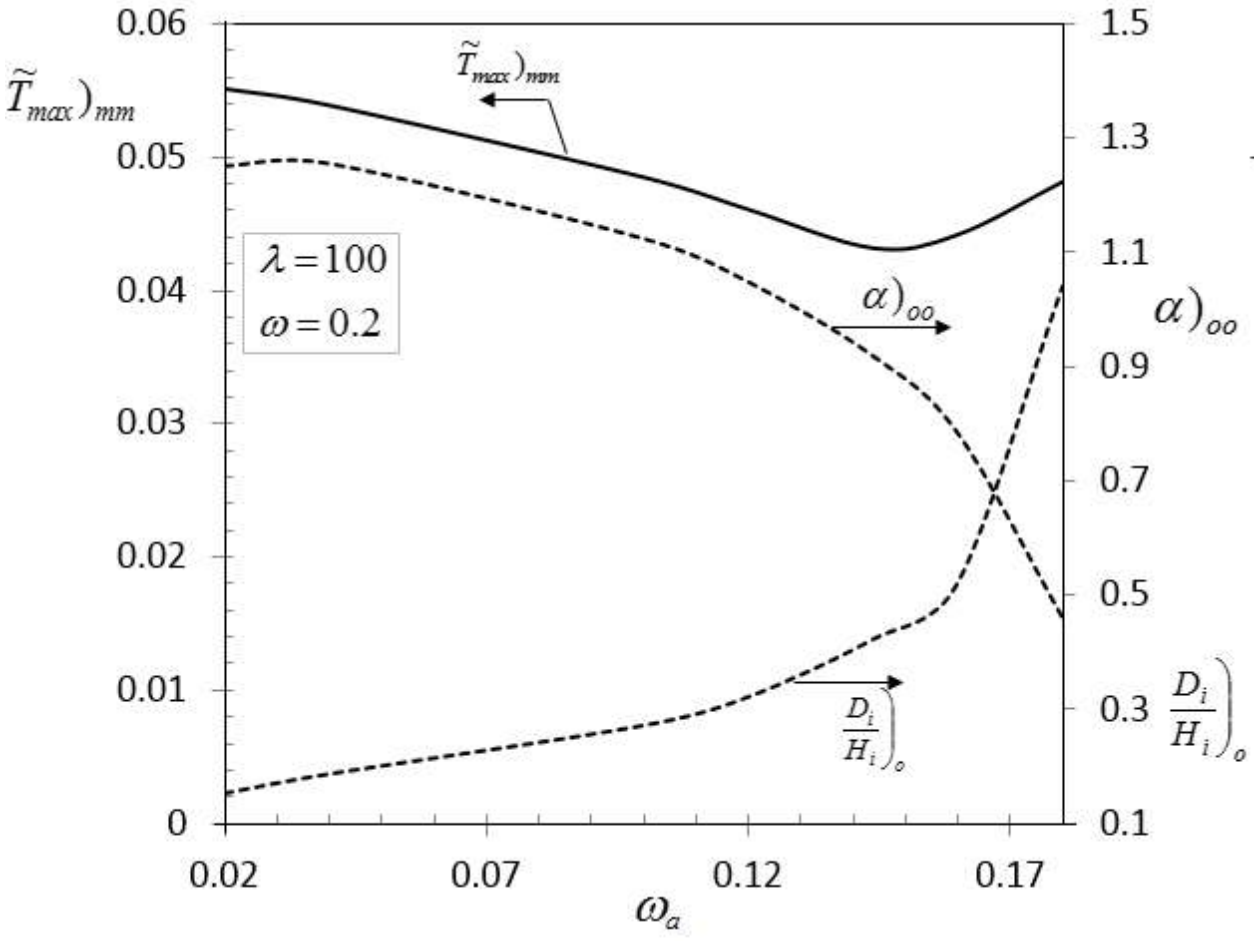


Figure 8 Influence of $\omega_a$ on the peak temperature of a heat generating body intruded by a V-shaped insert of 'V3' type.

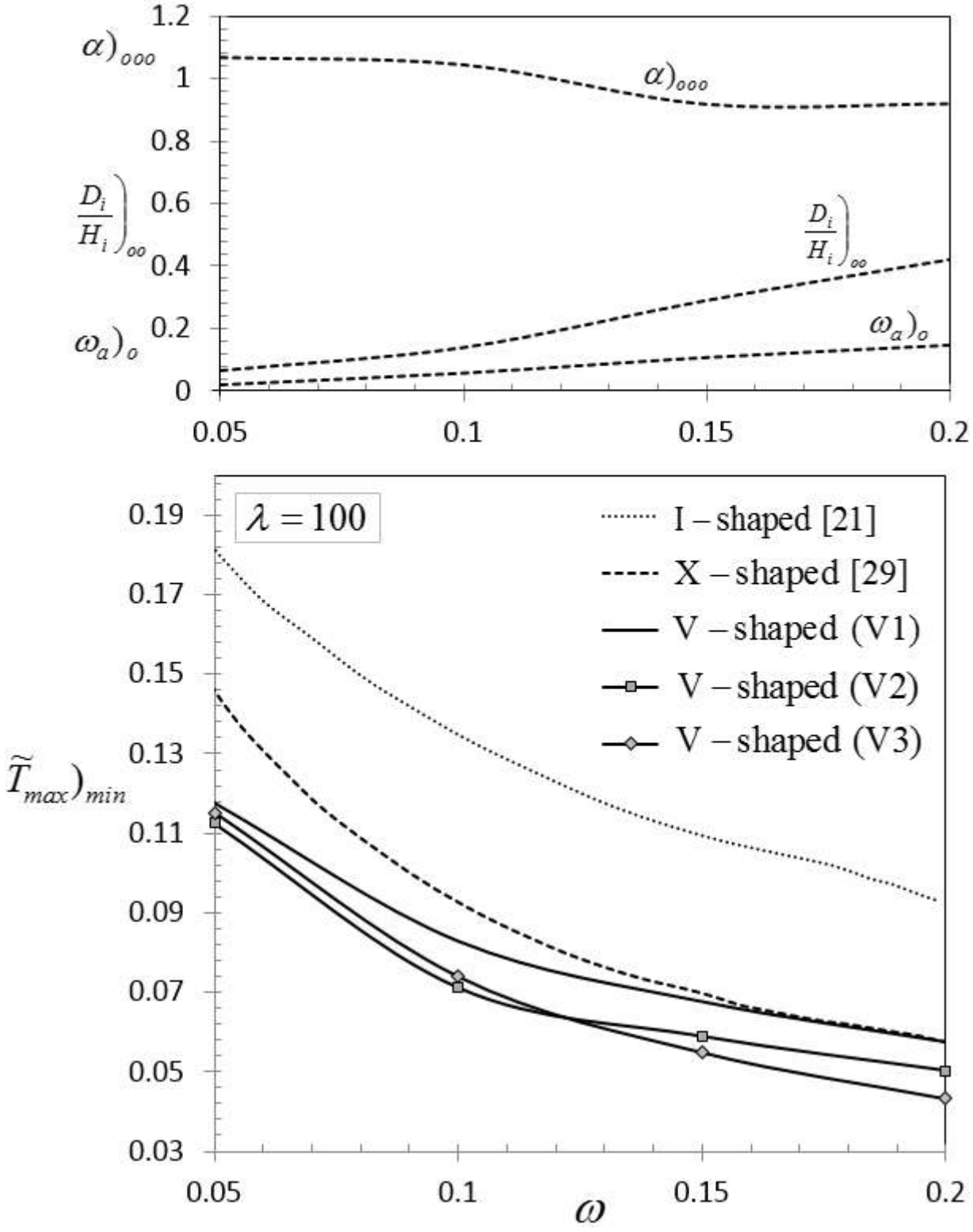


Figure 9 Comparison of 'V3' with other configurations.

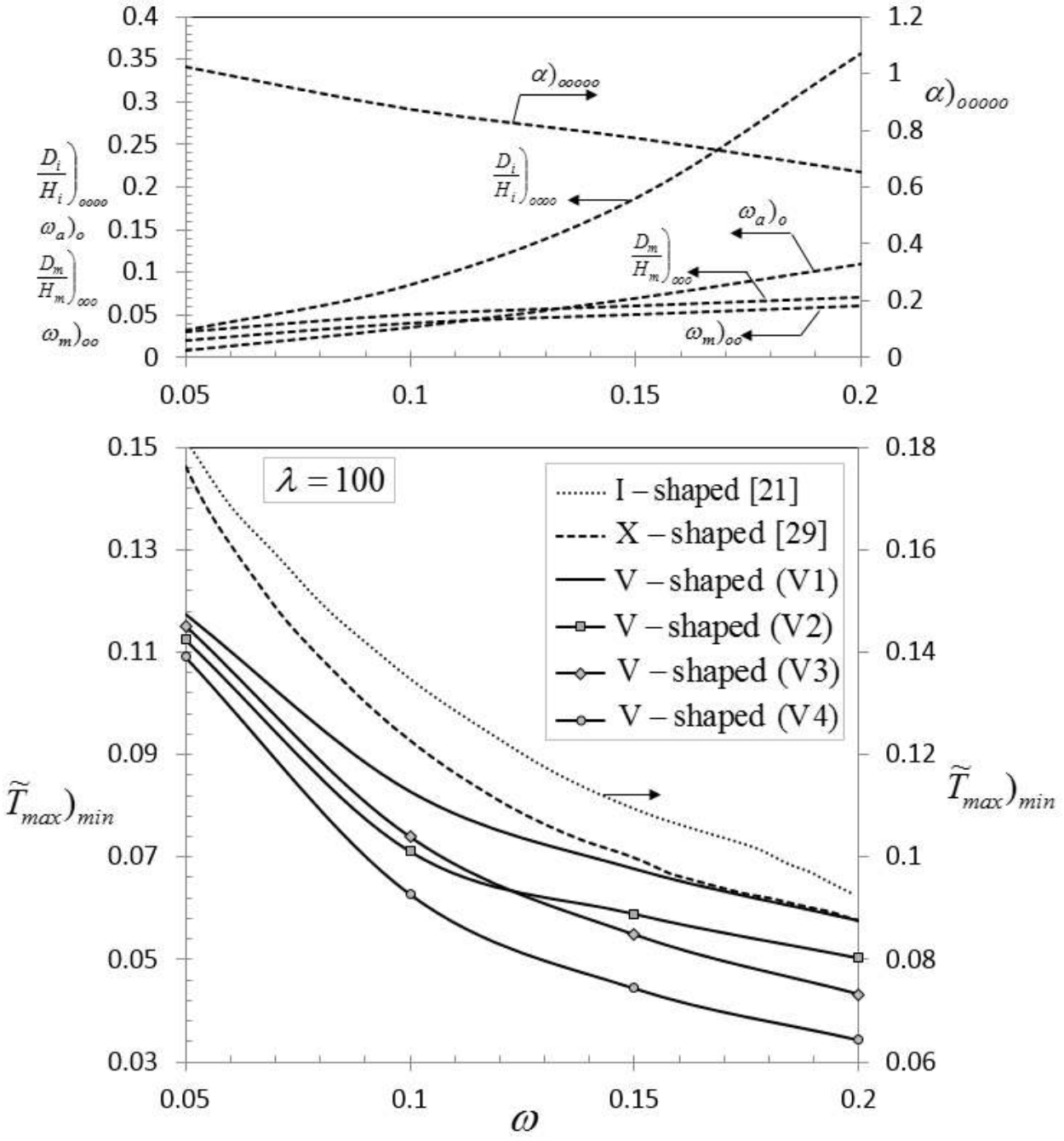


Figure 10 Comparison of 'V4' with other configurations.

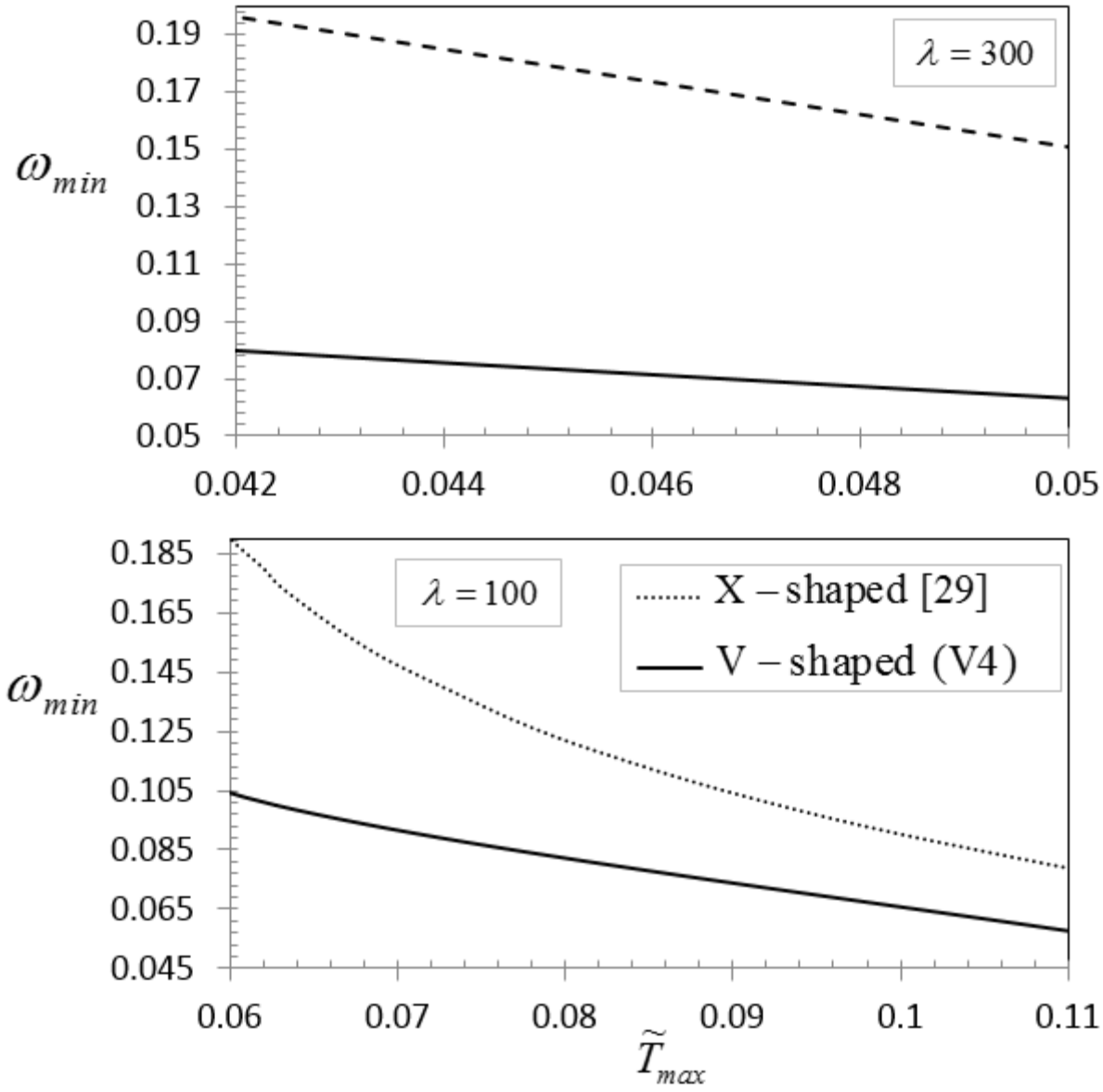


Figure 11 Minimum volume fraction required for maintaining the peak temperature of the heat generating body under an allowable level, $\tilde{T}_{max}$ .

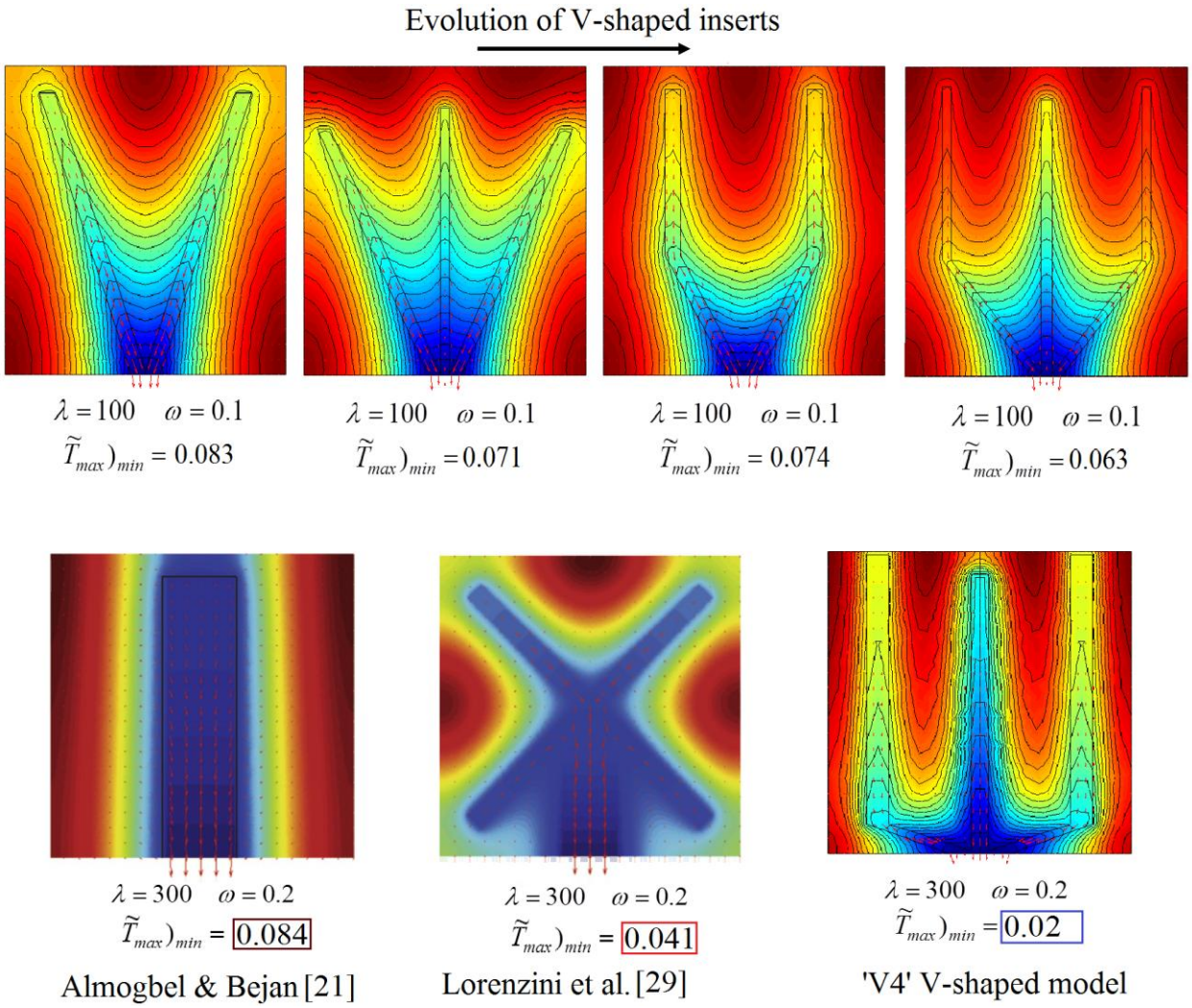


Figure 12 Optimal configurations of V-shaped inserts.